HHS Public Access

Author manuscript

*Results Chem*. Author manuscript; available in PMC 2025 January 10.

Published in final edited form as:

*Results Chem*. 2024 December ; 12: . doi:10.1016/j.rechem.2024.101882.

# Enhancement of antitumor effects of berberine chloride with a copper(II) complex against human triple negative breast cancer: *In vitro* studies

**Duaa R. Alajroush**[a], **Brittney F. Anderson**[b], **Janae A. Bruce**[b], **Christian I. Lartey**[a], **Dazonte A. Mathurin**[b], **Sean T. Washington**[a], **Tanaya S. Washington**[a], **Sidy Diawara**[a], **Sakariyau A. Waheed**[a], **Kaylin L. Thomas**[a], **Stephen J. Beebe**[c], **Alvin A. Holder**[a,*]

[a]Department of Chemistry and Biochemistry, Old Dominion University 4501 Elkhorn Avenue, Norfolk, VA 23529, USA

[b]Department of Biological Sciences, University of the Virgin Islands, 2 John Brewers Bay, St. Thomas, VI 00802, USA

[c]Frank Reidy Research center for Bioelectrics, Old Dominion University, 4211 Monarch Way, Suite 300, Norfolk, VA, 23508, USA

## Abstract

In this study, the copper(II) complex $[Cu(chromoneTSC)Cl_2]\cdot 0.5H_2O\cdot 0.0625C_2H_5OH$ (where chromoneTSC = *(E)-N*-Ethyl-2-((4-oxo-4H-chromen-3-yl)methylene)-hydrazinecarbothioamide) was synthesized and characterized; then used to carry out *in vitro* studies in combination with berberine chloride (BBC). The ligand and complex were characterized by elemental analysis, FTIR and NMR ($^1H$ and $^{13}C$) spectroscopy, and conductivity measurements. The cytotoxic effect was analyzed by using the CCK-8 viability assay in cancer MDA-MB-231 VIM RFP and non-cancer MCF-10A cell lines. The $IC_{50}$ values for the complex and BBC were 21.2 ±1.6 and 48.3 ± 2.4 μM, respectively at 24 h incubation, while the $IC_{50}$ value of the combination



*Corresponding author at: Department of Chemistry and Biochemistry, Old Dominion University 4501 Elkhorn Avenue, Norfolk, VA 23529, USA. aholder@odu.edu (A.A. Holder).

CRediT authorship contribution statement

**Duaa R. Alajroush:** Writing – review & editing, Writing – original draft, Validation, Methodology, Formal analysis, Data curation. **Brittney F. Anderson:** Methodology, Formal analysis, Data curation. **Janae A. Bruce:** Methodology, Data curation. **Christian I. Lartey:** Methodology, Formal analysis, Data curation. **Dazonte A. Mathurin:** Methodology, Formal analysis, Data curation. **Sean T. Washington:** Methodology, Formal analysis, Data curation. **Tanaya S. Washington:** Methodology, Formal analysis, Data curation. **Sidy Diawara:** Methodology, Formal analysis, Data curation. **Sakariyau A. Waheed:** Formal analysis, Methodology, Writing – review & editing. **Kaylin L. Thomas:** Formal analysis, Methodology, Writing – review & editing. **Stephen J. Beebe:** Writing – review & editing, Validation, Supervision, Resources, Formal analysis. **Alvin A. Holder:** Writing – review & editing, Visualization, Validation, Supervision, Software, Resources, Project administration, Investigation, Funding acquisition, Formal analysis, Data curation, Conceptualization.

Declaration of competing interest

The authors declare that they have no known competing financial interests or personal relationships that could have appeared to influence the work reported in this paper.

Appendix A. Supplementary data

Supplementary data to this article can be found online at https://doi.org/10.1016/j.rechem.2024.101882.

Appendix C. Supplementary data

Supplementary data to this article can be found online at https://doi.org/10.1016/j.rechem.2024.101882.

treatment was 9.3 ± 1.5 in cancer cells. The co-treatment group significantly increased the number of cells in G2 phase, indicating the growth arrest of cancer cells. Moreover, the combination group showed induction of both intrinsic and extrinsic apoptotic pathways. There was also a study on the effect of the combination treatment on receptor-interacting serine/threonine-protein kinase 3 (RIPK3) and mixed lineage kinase domain-like pseudokinase (MLKL) as biomarkers of necroptosis. The results showed activation of necroptosis after treatment with the combination of the copper complex and BBC *via* the activation of RIPK3–MLKL pathway.

### Keywords

Triple negative breast cancer; Berberine chloride; copper(II) complex; Thiosemicarbazones; Cell death mechanisms

## Introduction

Triple negative breast cancer (TNBC) is described as a subtype of breast cancer that expresses HER2 negatively as well as the estrogen and progesterone receptors [1]. Compared to most other forms of breast cancer, TNBC often grows more quickly and spreads more aggressively [2]. TNBC accounts for roughly 15–25% of all cases of breast cancer in young women under 40 years of age [3-5]. Patients with TNBC have shorter survival times than those with other subtypes of breast cancer, and their mortality rate is 40% in the first five years following diagnosis [6]. In non-TNBC patients, the average time to relapse is 35–67 months, whereas in TNBC patients, it is only 19–40 months. In the three months following recurrence, the mortality rate for TNBC patients can reach 75% [7,8].

Copper-containing complexes have potential applications, including as enzyme inhibitors, chemical nucleases, antimicrobials, antivirals, and anti-cancer agents [9]. In cancer cells, copper complexes that are believed to be less toxic than cisplatin have a different mechanism of action. Compared to other metals, the geometry of copper-containing complexes facilitates their interaction with the DNA helix [10]. A number of copper(II) based drugs under the trade name Casiopeinas® (Cas) were synthesized by Ruiz-Azuara *et al.* [11]. The general formula for these copper(II) complexes is $Cu(N\text{-}N)(X\text{-}X)NO_3$ (where N-N = phen, bpy, and analogues; while X-X = (N, O) or (O,O) donor ligands, acetylacetone or salicylaldehydate) [12-14]. The most successful drugs that have reached clinical trials in Mexico are Cas-II-gly and Cas-III-ia (see Fig. 1). The cytotoxic activity of these two complexes is a result of the activation of apoptosis through the generation of ROS, mitochondrial dysfunction, and cell cycle arrest. Also, they showed inhibition of cancer cell growth by DNA intercalation, cell migration, and cell proliferation inhibition [14].

In our society, natural products have been an enormous success for cancer treatment. Plants have historically been a useful source of effective anti-cancer agents [15]. Taxanes chemotherapeutic drugs, such as paclitaxel (Taxol) and docetaxel (Taxotere), as shown in Fig. 2, have shown anti-cancer effects. Taxol primarily works by inhibiting microtubule depolymerization, which prevents cancer cell division [16]. Furthermore, anthracyclines chemotherapeutic drugs, such as doxorubicin, daunorubicin, and epirubicin, as shown in

Fig. 2, are derived from *Streptomyces peucetius* var. *caesius*. They can be used to treat different types of cancer, including leukemia, lymphoma, breast cancer, uterine cancer, ovarian cancer, and lung cancer [17].

One of the cornerstones of cancer therapy is the combination of two or more therapeutic treatments to specifically target cancer-inducing or cell-sustaining pathways [18]. Combination therapy has an additive or synergistic effect, necessitating a lower therapeutic dosage of each drug [19]. It also has the potential to produce cytotoxic effects on cancer cells while simultaneously preventing toxic effects on healthy cells. This could happen if a drug in the combination regimen has a cytotoxicity interaction with another drug in normal cells that prevents the other drug from having cytotoxic effects on non-cancer cells, necessitating a lower therapeutic dosage of each drug [20].

Many studies investigated that alkaloids and cisplatin treatment can prevent damage to non-target organs, such as the kidney, liver, and the nervous system, from cisplatin damage by blocking some pathways [21]. The antiproliferative potential of various isoquinoline alkaloids (see Fig. 3) was demonstrated by inhibiting the biosynthesis of RNA, DNA, and proteins [22]. They also showed induction of autophagy and apoptotic pathway through the up- and down-regulation of various proteins [23]. Among the isoquinoline alkaloids, berberine (Fig. 3) was isolated from a variety of medicinal plants, including *Berberis vulgaris* (barberry), *Berberis aristata* (tree turmeric), *Coptis chinensis* (Chinese goldthread), *Hydrastis canadensis,* and *Phellondendron amurense*. Berberine showed anti-cancer and antimetastatic activities against various cancers, such as lung, cervix, breast, and prostate cancer both *in vitro* and *in vivo* [24].

Berberine was studied in combination with cisplatin to treat cancers with fewer side effects. Youn *et al.* [25] studied the effect of the combination of berberine and cisplatin toward human cervical cancer HeLa cells. The results showed a significant decrease in cell survival in comparison with berberine or cisplatin treatment alone. Berberine showed a significant cytotoxic effect at a dose of 50 μg/mL, however, its toxicity was enhanced by around 54% when combined with 5 μM of cisplatin. The combination treatment caused a decrease in the mitochondrial membrane potential, leading to the release of cytochrome *c*, resulting in activation of caspases and apoptosis [25]. A study by Zhao *et al.* [26] showed a high anti-cancer effect of combination treatment between berberine (BBR) and cisplatin in breast cancer MCF-7 cells. The $IC_{50}$ value of berberine was 52.178 ± 1.593 μM, and the $IC_{50}$ value of cisplatin was 49.541 ± 1.618 μM. Berberine increased the sensitivity of MCF-7 cells to cisplatin in a dose and time-dependent manner. When cisplatin was combined with 26 μM of berberine, the $IC_{50}$ value was 5.759 ± 0.76 μM [26].

In our efforts to investigate the anti-cancer effects of copper-containing thiosemicarbazone complexes, we synthesized $[Cu(chromoneTSC)Cl_2]•0.5H_2O•0.0625C_2H_5OH$. Herein, we investigated the cytotoxic effect of the copper(II) complex in combination with berberine chloride (BBC) on a human TNBC cell line, MDA-MB-231 VIM RFP, and a human non-cancer breast epithelial cell line, MCF-10A. Studies of induction of apoptosis and necroptosis along with the effect on the cell cycle arrest were also discussed.

# Experimental

## Reagents and instrumentation

All chemicals and reagents were purchased from commercial sources for *in vitro* studies to treat TNBC cells. Eagle's Minimum Essential Medium (EMEM), fetal bovine serum (FBS), Dulbecco's Modified Eagle Medium (DMEM), and horse serum were obtained from Mediatech, Inc. (Manassas, VA). Cell Counting Kit-8 (CCK-8) assay kit was obtained from Dojindo. Caspase-8 Glo® assay, Caspase-9 Glo® assay, and Caspase-3/7 Glo® assay kits were purchased from Promega Corporation (Madison, WI). CellEvent™ Caspase-3/7 Green flow cytometry assay kit, DAPI (4′,6-diamidino-2-phenylindole) blue-fluorescent DNA stain, Goat anti-Rabbit IgG (H + L) Highly Cross-Adsorbed Secondary Antibody Alexa Fluor™ Plus 488, Pierce™ BCA protein assay kit, and GAPDH Monoclonal Antibody (6C5) were purchased from ThermoFisher Scientific. Phospho-RIP3 (Ser227) (D6W2T) and phospho-MLKL (Ser358) (D6H3V) Rabbit mAb were obtained from Cell Signaling Technology. Precision Plus Protein™ Dual Color Standards was obtained from Bio-Rad. Berberine chloride was purchased from Sigma-Aldrich.

All FTIR spectra were acquired on a Thermo© Nicolet Avatar 370 DTGS (FT IR/ATR IR) spectrophotometer and Bruker Platinum ATR-IR spectrometer. Elemental analysis for carbon, hydrogen, and nitrogen was acquired on a Thermo Scientific FLASH 2000 Organic Elemental analyzer. All UV–visible spectra were acquired on an Agilent 8453A diode array spectrophotometer, while all conductivity measurements were acquired on a SPER Scientific 860,032 benchtop conductivity/TDS/salinity meter.

Electrospray ionization mass spectrometry (ESI MS) spectra were acquired via positive electrospray ionization on a Thermo Scientific LTQ XL ESI MS system, equipped with an LTQ Ion Trap/Orbitrap XL ion source, located in the Department of Chemistry and Biochemistry, Old Dominion University, Norfolk, VA 23529, U.S.A. Methanol (99% purity) was introduced into the capillary system at a flow rate of 10 mL $min^{-1}$. A background scan was acquired to establish a baseline. The methanolic solution with the dissolved copper(II) complex was injected directly into the mass spectrometer via a syringe connected to the capillary system; then the mass spectrum was acquired. The data was then processed by using the X-Calibur Qual and Origin Version 7.0 software.

All NMR spectra were acquired on a Bruker 400 MHz spectrometer with DMSO-$d_6$ as a solvent and were processed using ACD/NMR Processor Academic Edition and BRUKER topspin software. Flow cytometry data was acquired on a Miltenyi MacsQuant Analyzer 10 flow cytometer. Absorbance and luminescence were acquired on a SpectraMax i3 microplate reader. The ChemiDoc™ MP Imaging System (Bio-Rad) instrument was used to photograph western blot bands. The immunofluorescence images were taken with a LEICA DMi8 microscope and analyzed by using the Leica LAS X software.

## Synthesis of ligands and complexes

**Synthesis of chromoneTSC•0.25$C_2H_5OH$—**This was synthesized by following the procedure as reported in the literature [27]. Chromone-3-carboxaldehyde (3.43 g, 19.7 mmol) and 4-ethyl-3-thiosemicarbazide (2.35 g, 19.7 mmol) were added to a 250 mL round

bottom flask; then absolute ethanol (100 mL) was added. Approximately 10 drops of glacial acetic acid were added to the off-white suspension and the reaction mixture was refluxed for three hours. The reaction mixture was then cooled to room temperature; then filtered through a sintered glass crucible. The yellow solid obtained was washed with ethanol (3 x 15 mL), followed by ether (3 x 10 mL), and allowed to air dry. The filtrate was evaporated to a minimum volume, to leave a precipitate, which was then filtered off and collected after being washed with ethanol and air dried. Yield = 4.67 g (86%). Calc. for $C_{11}H_9N_3O_2S$: C, 56.35; H, 5.10; N, 14.65. Found: C, 56.03; H, 4.67; N, 14.52. $^1$H NMR (400 MHz, DMSO-$d_6$, δ/ppm): 11.65 (s, 1 H, N-NH-CS), 9.13 (s, 1 H, CH=N), 8.59 (t, $J$ = 5.8 Hz, 1 H, NH-$C_2H_5$), 8.19 (s, 1 H, O-CH). $^{13}$C NMR (400 MHz, DMSO-$d_6$, δ/ppm): 177.2 (C=S), 175.3 (C=O), 156.2 (C-O), 155.4 (C=N). FTIR ($\nu$ / cm$^{-1}$): 3328 (w) (−N$^1$H), 3230 (m) (−N$^2$H), 1632 (vs) (C=O), 1531 (vs) (C=N), 1341 (s) (C-O), and 1214 (vs) (C=S).

Lit.[27] $^1$H NMR (400 MHz, DMSO-$d_6$, δ/ppm): 11.50 (s, 1 H, N-NH-CS), 9.08 (s, 1 H, CH=N), 8.59 (t, $J$ = 5.8 Hz, 1 H, NH-$C_2H_5$), 8.15 (s, 1 H, O-CH). $^{13}$C NMR (400 MHz, DMSO-$d_6$, δ/ppm): 177.0 (C=S), 175.3 (C=O), 156.1 (C-O), 155.4 (C=N). FTIR ($\nu$ / cm$^{-1}$): 3363 (w) (−N$^1$H), 3230 (m) (−N$^2$H), 1634 (vs) (C=O), 1541 (vs) (C=N), 1344 (s) (C-O), and 1221 (vs) (C=S).

**Synthesis of [Cu(chromoneTSC)Cl$_2$]•0.5H$_2$O•0.0625C$_2$H$_5$OH—**This complex was prepared for the very first time by following the respective synthetic procedure. The ligand, chromoneTSC•0.25$C_2H_5OH$ (0.281 g, 0.001 mmol), and anhydrous $CuCl_2$ (0.138 g, 1.03 mmol), along with anhydrous ethanol (100 ml) and a trace of DMF, were mixed in a 250 RB flask; then refluxed for two hours. The reaction mixture was cooled to RT; then, the resulting green mixture was filtered to recover the green product. The green residue was washed with anhydrous ethanol, followed by anhydrous ether, then air dried. Yield = 0.321 g (78%). Calc. for $C_{13}H_{13}C_{12}CuN_3O_2S$: C, 37.39; H, 3.44; N, 9.97. Found: C, 37.42; H, 3.10; N, 9.60. FTIR ($\nu$ / cm$^{-1}$): 3189 (w) (−N$^1$H), 2988 (m) (−N$^2$H), 1630 (vs) (C=O), 1583 (vs) (C=N), 1479 (s) (C-O), and 1344 (vs) (C=S). Conductivity measurements (a 1 mM solution): In DMSO, $\wedge_m = 6.6\ \mu S\ cm^{-1}$.

## Cell culture

**MDA-MB-231 VIM RFP cell line—**MDA-MB-231 VIM (vimentin) RFP (red fluorescent protein) reporter TNBC cell line is fibroblast-like breast adenocarcinoma cell that was isolated from the pleural effusion of a 51-year-old, White, female TNBC cells. The MDA-MB-231 VIM RFP cells were obtained from American Type Culture Collection (ATCC). These cells were cultured in Eagle's Minimum Essential Medium (EMEM) that was supplemented with 10% fetal bovine serum (FBS), 0.01 mg ml$^{-1}$ human recombinant insulin, and 10 μg ml$^{-1}$ blasticidin S HCl, 1% penicillin/streptomycin, and incubated at 37 °C in 5% $CO_2$.

**MCF-10A cell line—**MCF-10A cells (non-tumorigenic human cell line from human breast epithelial cells) were obtained from American Type Culture Collection (ATCC). MCF-10A cells were cultured in Dulbecco's Modified Eagle Medium (DMEM) with 5% horse serum, 20 ng ml$^{-1}$ epidermal growth factor (EGF), 0.5 μg ml$^{-1}$ hydrocortisone, 100 ng ml$^{-1}$ cholera

toxin, 10 μg $ml^{-1}$ insulin, and 1% penicillin/streptomycin, and incubated at 37 °C in 5% $CO_2$.

## Cytotoxicity study

The cells were seeded in a 96-well clear-bottom plate at a concentration of $1.5 \times 10^4$ cells/well. The complexes were added to the cells at different concentrations (0–100 μM). Following the administration of the drugs, three plates were incubated for 24, 48, and 72 h, respectively. After incubation, the cells were assayed for viability using CCK-8 assay by adding the WST-8 reagent and measuring the absorbance at 450 nm. The Origin 7.0 software was used to analyze the data and to determine the $IC_{50}$ values.

## Cell death mechanism studies

**Detection of apoptotic cell death—**MDA-MB-231 VIM RFP cells were plated at a concentration of $3 \times 10^5$ cells/mL and incubated for 24 h. The cells were treated with the $IC_{50}$ values of the complexes. The CellEvent™ Caspase-3/7 green reagent (2 μL) was added at different time points to 100 μL of samples. Then the samples were incubated for 25 min at 37 °C, 5% $CO_2$ and protected from light. The VIM-RFP in cells and the caspase 3/7 green fluorescent were collected at 532/588 and 511/533 nm, respectively by flow cytometry.

Caspase 8 and 9 activities were analyzed to investigate the apoptotic pathways induced by the complexes to kill cancer cells since caspase 8 is involved in the extrinsic pathway and caspase 9 in the intrinsic pathway by using Caspase-Glo® 8 and 9 assay kits. The MDA-MB-231 VIM RFP cancer cells were seeded on a 96-well plate ($1.5 \times 10^4$ cells/well) in 100 μL of medium. The cells were treated with the $IC_{50}$ value of the complexes. Then the reagent of the assays was added to each sample, and the reaction mixtures were mixed by a plate shaker at 300–500 rpm for 30 s. The luminescence was read in a microplate reader after 1 h incubation at room temperature.

**Cell cycle analysis—**The cell cycle was evaluated by flow cytometry using DAPI staining on a flow cytometer. The cancer MDA-MB-231 VIM RFP cells were plated at a concentration of $1 \times 10^6$ cells/mL in a 6-well plate, treated with the $IC_{50}$ values of the compounds for 24 h. Then cells were washed in phosphate buffered saline (PBS), resuspended with ice-cold 70% EtOH, stored in fixative at 4 °C for 2 h. Then cells were washed in PBS, resuspended in staining solution. Experiments were performed in triplicate. G1, S, and G2 fractions were quantified with the FlowJo software.

## Detection of necroptotic cell death mechanism

**Immunofluorescence assay.—**The cancer cells were plated in 4-well chamber slides and treated with the $IC_{50}$ values of the compounds for 24 h. The cells were fixed with 4% paraformaldehyde at room temperature for 15 min and washed 3 times with 1X PBS. The cells were permeabilized with 0.1% Triton-X 100 and incubated with 2% blocking solution bovine serum albumin (BSA) at room temperature Antibodies against p-RIPk3 and p-MLKL in primary antibodies diluent (0.1% BSA) were added and incubated at 4 °C overnight. The cells were incubated with the Alexa Fluor™ Plus 488 secondary antibody at room

temperature for 1 h and washed 3 times with PBS. DAPI stain was used for counterstain. Images were obtained with a fluorescence microscope.

**Western blot analysis.—**The cancer cells were plated at a concentration of $1 \times 10^6$ cells/mL in a 6-well plate. Then the cells were treated with the $IC_{50}$ values of compound and incubated for 24 h. The treated cells were lysed to extract proteins by adding RIPA lysis buffer. Then, the total protein concentration of cell lysate was determined by using the BCA assay. The samples containing equal amount of proteins were loaded into 10% SDS-PAGE wells. The electrophoresis was set up for 2 h at 100 V to separate the proteins based on their molecular weight. After electrophoresis, the proteins were transferred into a nitrocellulose membrane, which was placed into a transfer cassette to run for 90 min at 60 V. After transfer, the membrane was incubated in tris-buffered saline (TBS) blocking solution for 30 min to prevent non-specific binding of antibodies. The membrane was incubated with the primary antibodies (p-MLKL and GAPDH) overnight at 4 °C, then incubated with the secondary Alexa Fluor™ Plus 488 antibody for 1 h at room temperature. Lastly, the membrane was photographed, and the bands were measured with the ImageJ software.

### Statistical analysis

The FlowJo software was used for analyzing flow cytometric data. Origin 7.0 software was used to plot the graphs for all cytotoxic studies and to determine the $IC_{50}$ values. ImageJ software was used to analyze the bands in the western blot study. GraphPad Prism 9 software was used for statistical analyses namely one-way and/or two-way analysis of variance between groups. All experiments were conducted at least three times and data were expressed as mean ± standard error (S.E.). Asterisks represent P values of < 0.05 “*”, <0.01 “**”, <0.001 “***”, <0.0001 “****.

## Results and discussions

### Synthesis and characterization of chromoneTSC•0.25$C_2H_5OH$

The ligand was synthesized by following the procedure as reported by Haribabu *et al.* [27]. The synthesis is shown in Scheme 1.

**Elemental analysis of the “free” ligand, chromoneTSC•0.25$C_2H_5OH$—**Elemental analysis was carried out on the chromoneTSC•0.25$C_2H_5OH$ ligand. The carbon, hydrogen, and nitrogen percentages were found as 56.03%, 4.67%, and 14.5%, respectively, while the calculated percentage were 56.35%, 5.10%, and 14.65%, respectively. The elemental analysis data confirmed that chromoneTSC•0.25$C_2H_5OH$ ligand was pure on isolation.

**$^1$H and $^{13}$C NMR spectroscopic analysis of the ligand, chromoneTSC•0.25$C_2H_5OH$—**The ligand was previously synthesized and characterized as reported by Haribabu *et al.* [27]. The $^1$H NMR spectrum of the ligand exhibited signals occurred at 11.50 and 8.59 δ/ppm, which corresponded to thioamide and terminal NH protons, respectively [27]. The $^1$H NMR spectrum of the ligand showed peaks at 11.65 and 8.59 δ/ppm which accounted for N-NH-CS and NH-$C_2H_5$, respectively as shown in Fig. 4. Moreover, an azomethine proton was observed at 9.13 δ/ppm as a singlet in the spectrum of

the ligand. This is in line with the previous report of the same ligand which was a single at 9.08 δ/ppm for the CH=N [27]. Another signal located at 8.19 δ/ppm in the spectrum of the ligand for the O-CH functional group. Based on spectroscopic data available in the literature, this signal is inferred to be due to the OCH proton of the chromone moiety [27].

Moreover, the $^{1}$H NMR spectrum showed signals occurred at 7.82, 7.68, and 7.52 δ/ppm, which corresponded to the protons of the aromatic ring of the chromone moiety. Other peaks at 2.50 at 1.14 δ/ppm were observed for $NHCH_2$ and $CH_2CH_3$ as shown in the literature [27]. Our $^{1}$H NMR spectroscopic data were matched the spectra of the same ligand in previous literatures [27-30], indicating the purity of the chromoneTSC•$0.25C_2H_5OH$ ligand.

In the $^{13}$C NMR spectrum of the ligand, the peaks due to C=S, C=O, C-O, and C=N carbons occurred at 177.0, 175.3, 156.1, and 155.4 δ/ppm, respectively, as reported in literature [27]. Our $^{13}$C NMR spectrum showed peaks at 177.2, 175.3, 156.2, and 155.4 δ/ppm which accounted for C=S, C=O, C-O, and C=N, respectively as shown in Fig. 5. Moreover, the $^{13}$C NMR spectrum exhibited other signals at 135.0, 134.2, 126.5, 125.6, and 123.7 δ/ppm which are related to the carbons in the aromatic ring of chromone moiety as reported in the literature [27]. These spectroscopic data were similar to the reported spectra of the same ligand in the literature [27-30], thus indicating the purity of the chromoneTSC•$0.25C_2H_5OH$ ligand.

**FTIR spectroscopic analysis of the "free" ligand, chromoneTSC•$0.25C_2H_5OH$**—FTIR spectrum of the ligand exhibited stretching frequencies of 3328 and 3230 $cm^{-1}$, as designated for $\nu(N^1H)$ and $\nu(N^2H)$, respectively, as shown in Fig. 6. When compared to a literature [27], the FTIR spectrum exhibited bands at 3363 and 3230 $cm^{-1}$, which were assigned to terminal and thioamide NH groups, respectively [27]. In our experimental FTIR, the spectrum showed stretching frequencies assigned to the $\nu(C = O)$ and $\nu(C = N)$ occur at 1632 and 1531 $cm^{-1}$. Moreover, the ligand exhibited a stretching frequency at 1214 $cm^{-1}$ for $\nu(C = S)$. This is similar to the previous report of the same ligand with stretching frequencies at 1634, 1541, and 1221 $cm^{-1}$ for C=O, C=N, and C=S functional groups. The FTIR spectra were compared and matched the stretching frequencies as observed in the literature [27-30], indicating that chromoneTSC•$0.25C_2H_5OH$ ligand was pure.

## Synthesis of [Cu(chromoneTSC)$Cl_2$]•$0.5H_2O$•$0.0625C_2H_5OH$

The complex was prepared for the very first time as shown in Scheme 2.

**Elemental analysis of the complex, [Cu(chromoneTSC)$Cl_2$]•$0.5H_2O$•$0.0625C_2H_5OH$—**Elemental analysis was carried out on the complex. The calculated percentages for carbon, hydrogen, and nitrogen were 37.39%, 3.44%, and 9.97%, respectively. The percentage for carbon, hydrogen, and nitrogen were found as 37.42%, 3.1%, and 9.6%, for the complex, with the complex having $0.5H_2O$ and $0.0625C_2H_5OH$ as solvates. The elemental analysis data confirmed the identity and purity of the complex.

**FTIR spectroscopic analysis of the "free" ligand and the complex—**According to the FTIR spectra results, as shown in Fig. 7, the complex exhibited stretching frequencies of 3189 and 2988 $cm^{-1}$, as designated for $\nu(N^1H)$ and $\nu(N^2H)$, respectively. Table 1 summarize the FTIR spectra of the chromoneTSC•$0.25C_2H_5OH$ ligand and the complex. A strong stretching frequency assigned to the $\nu(C = N)$ in the spectrum occur at 1531 $cm^{-1}$ for the "free" ligand but shifted to 1583 $cm^{-1}$ in the FTIR spectrum of the complex. A stretching frequency was observed at 760 $cm^{-1}$ for $\nu(C = S)$ for the "free" ligand, while it was shifted to a higher stretching frequency of 802 $cm^{-1}$ when the ligand was coordinated to the copper(II) metal center.

**Molar conductivity measurements of the complex—**Conductivity measurement was carried out on a 1.0 mM DMSO solution of the complex. The value was determined for the complex with $\wedge_m = 6.6\ \mu S\ cm^{-1}$. This low value indicated that the complex in DMSO was a non-electrolyte based on the use of conductivity measurements to ascertain types of electrolytes in various solvents as reported by Geary [31].

**Mass spectral analysis of the complex—**To complement the elemental analysis of the complex, it was necessary to show the ESI MS data (not including the solvates) which showed a mononuclear species (species A), which was detected with a *m/z* value of 336.94 (Fig. S1). Also, an *m/z* value of 710.700 (Fig. S1) of which has a proposed binuclear species (species B) was detected from a methanolic solution.

Figure S2 shows a plausible mechanism of how two species were formed, along with their formulae as detected in the chamber of the mass spectrometer. In the mononuclear (species A) and binuclear species (species B), the chromoneTSC ligand was found to coordinate as a thiolate anion while being detected in the positive mode while in the chamber of the mass spectrometer (Fig. S2). This is due to the fact that thiosemicarbazones ligands can exist as thione–thiol tautomers (although the proton lost to form the anion formally belongs to the hydrazinic–NH group) [32-34]. Such thiosemicarbazones can undergo tautomerisation and subsequent deprotonation of the thiol form allowing for a mono-anionic ligand [32-34].

On a note, it is believed *m/z* value at 603.98 could be due to either an unknown species or from the background which has an appreciable intensity.

## In vitro studies

**Cytotoxicity studies—**There have been reports of the anti-cancer activity of berberine as a natural product and its combination with cisplatin [21]. In this study, to determine the potential anti-cancer activity of the Cu(II) complex and berberine chloride (BBC) in combination, we firstly treated the cancer MDA-MB-231 VIM RFP and non-cancer MCF-10A cells with increasing concentrations (0–100 μM) of the Cu(II) complex or BBC for different hours (24, 48, and 72 h). Cell viabilities were measured and quantified by the CCK-8 assay. The results obtained show that the Cu(II) complex or BBC alone significantly inhibited cancer cell viability in a dose-dependent manner at 24 h incubation. The $IC_{50}$ value of BBC was 48.3 ± 2.4 μM at 24 h, and therefore the concentration of 50 μM was chosen as the optimal BBC concentration in the cell viability study of combination treatment. The

cells were treated with different concentrations of the Cu(II) complex with 50 μM of BBC to study the cytotoxic effect of the complex when it combined with berberine chloride. Our data showed that the combination treatment increased the toxicity of the Cu(II) complex against the cancer cells following 24, 48, and 72 h incubations as shown in Fig. 8. This indicates the potential anti-cancer effect of co-treatment of the complex and BBC when compared to the groups of a single treatment.

Table 2 shows a tabulation of the $IC_{50}$ values in MDA-MB-231 VIM RFP cells after treatment with the Cu(II) complex and/or BBC. The cytotoxic effect of co-treatment of the Cu(II) complex and BBC was significantly higher than that of either the complex or BBC alone and cisplatin as well, giving the lowest $IC_{50}$ values following 24, 48, and 72 h incubations. The $IC_{50}$ values for the Cu(II) complex and BBC were 21.2 ± 1.6 and 48.3 ± 2.4, respectively at 24 h incubation, therefore 20 μM of the Cu(II) complex and 50 μM of BBC were chosen in the following experiments.

The cancer cell viability after the combination treatment with the Cu (II) complex (20 μM) and BBC (50 μM) was significantly lower than that of single treatment at 24, 48, and 72 h as shown in Fig. 9. Berberine could improve the sensitivity of MDA-MB-231 VIM RFP cancer cells to the Cu(II) complex treatment. The combined action between the Cu(II) complex and BBC produced a more potent and effective anti-cancer response when compared to using either drug alone. These data are in line with previous reports showing that berberine exhibited antiproliferation activity against TNBC cells. A study investigated the anti-cancer activity of berberine on two TNBC lines, including MDA-MB-231 and BT549. The viability of cells after 48 h of treatment with berberine giving $IC_{50}$ of 16.575 ± 1.219 μg $mL^{-1}$ and 18.525 ± 6.139 μg $mL^{-1}$ in BT549 and MDA-MB-231 cells, respectively [35]. Berberine in combination with cisplatin previously showed a prominent inhibitory effect on cancer cell growth when compared to the single treatment [36].

In non-cancer cells, BBC showed a low cytotoxic effect giving high $IC_{50}$ values (>100 μM) at 24 and 48 h and (92.3 ± 1.4 μM) at 72 h, as shown in Table 3. Studies have shown that berberine has an antiproliferative effect against a variety of human cancer cells and is less toxic toward non-cancer cells. *In vitro* study by Sudheer *et al.* [37]. demonstrated that the treatment of non-cancer human prostate epithelial cells with berberine (10–100 μM) did not show a significant cytotoxic effect [37]. Another study reported the cytotoxic effect of a high dose of berberine (500–600 times more than human dosage) in pregnant rats. There was no significant reproductive toxicity related to berberine found in the results [38].

On the other hand, the toxicity of the Cu(II) complex in combination with 50 μM of BBC was significantly decreased when compared to that of the complex treatment alone following 24, 48, and 72 h incubations as shown in Fig. 10. The $IC_{50}$ values of a co-treatment group of the Cu(II) complex and BBC as compared with the groups of a single treatment, were significantly higher than its $IC_{50}$ in the breast cancer cell line as shown in Table 3. The $IC_{50}$ value of the Cu(II) complex at 24 h incubation in non-cancer MCF-10A cells was 58.7 ± 2.1 μM, which is around three times higher than its $IC_{50}$ (21.2 ± 1.6 μM) in cancer MDA-MB-231 VIM RFP cells. While the $IC_{50}$ value of the combination between the Cu(II) complex and BBC in non-cancer cells was 94.5 ± 1.8 μM, which is around ten times higher

than its $IC_{50}$ (9.3 ± 1.5 μM) in cancer cells. This implies that the combination treatment between the Cu(II) complex and BBC has more selectively cytotoxic effect to the TNBC than the treatment with the complex alone.

Since cancer is a heterogeneous disease with multiple interacting signaling pathways contributing to its initiation, promotion, and progression, multitargeted drugs are expected to have a more effective mechanism of action against cancer than single-targeted ones. Furthermore, it has been reported that single-targeted compounds can activate interrelated signaling pathways to block rationally targeted pathways, thereby increasing cell proliferation [39]. In order to investigate the mechanisms underlying the inhibition of cancer cell viability between BBC and the complex, we examined different cell death mechanisms including cell cycle arrest, apoptosis, and necroptosis as described below.

## Cell death mechanisms

**Cell cycle studies.—**Cell cycle arrest is an important mechanism to inhibit cancer cell growth, and it was reported that many chemotherapeutic drugs act on targeting the cell cycle and inhibition cancer cell division. To determine whether the Cu(II) complex and berberine chloride affected the cell cycle of the cancer MDA-MB-231 VIM RFP TNBC cells, cell cycle analysis was assessed by flow cytometry. The cells were treated with the $IC_{50}$ values of the complex and/or BBC for 24 h, then stained with DAPI solution. The results showed a significant decrease in G1 phase after treatment with the Cu(II) complex, BBC, and combination therapy as shown in Fig. 11. Moreover, the results showed that the BBC and co-treatment group significantly increased the number of cells in the G2 phase when compared to the untreated group as shown in Fig. 12. This indicates the increase in the growth arrest of cancer cells in G2 phase with 38.4% for co-treatment of the Cu(II) complex and BBC compared to 23.2% and 33.8% for the complex or BBC alone, respectively. The high percentage of cells at the G2 phase indicates the prevention of cells from entering the mitosis phase, which leads to the inhibition of cancer cell division into two daughter cells. It was reported that berberine can inhibit the proliferation of prostate cancer PC3 cells by the induction of G0/G1 or G2/M phase arrest. The treatment with 10 μM of berberine induced G0/G1 cell cycle arrest, while the concentration of 50 μM inhibited the cell cycle at G2/M phase. The authors suggest that the treatment of PC3 cells with diverse concentrations of berberine activated different cell cycle signaling pathways [40].

The copper(II) complex, however, showed a high percentage of cells in the S phase when compared to the untreated group indicating the inhibition of DNA synthesis during the cell cycle. Copper(II)-thiosemicarbazone complexes have been reported to inhibit cancer cell growth by the inhibition of cell cycle at S phase. Zhang *et al.* [41] reported the mechanism of action of a copper complex with 8-hydroxyquinoline-2-carboxaldehyde-4,4-dimethyl-3-thiosemicarbazide in cisplatin-resistant neuroblastoma cells. The results exhibited a strong cell growth inhibition by the induction of S phase cell cycle arrest, suggesting the inhibition of DNA synthesis [41]. It has been reported that thiosemicarbazones and their derivatives can inhibit cancer cell proliferation by the inhibition of ribonucleotide reductases or DNA polymerase [42,43]. Another study reported that copper bis(thiosemicarbazone) complexes

caused inhibition of cell cycle progression of Ehrlich ascites carcinoma (EAC) cells in S phase [44].

Our study showed that the combination of berberine chloride and the Cu(II) complex arrested TNBC cell proliferation at the G2 phase. We suggest that BBC enhanced the DNA damage in the S phase which is caused by the Cu(II) complex leading to an increase in the suppression of breast cancer cell division in G2 phase. The inhibition of the cell cycle through different phases by each drug increases the potential anti-cancer activity in the combination case that occurred by the co-treatment of the Cu(II) complex and BBC.

## Apoptotic mode of cell death

**Caspase 3/7 activity.—**Caspase 3/7 was detected by the CellEvent™ Caspase-3/7 Green flow cytometry assay. The MDA-MB-231 VIM RFP cells were treated with the $IC_{50}$ value of the complex and/or BBC for 24 h. Then caspase 3/7 reagent was added, and the green fluorescent was collected at 511/533 nm, by flow cytometry. The results of the complex showed around 26% of cells that activated caspase 3/7 as shown in Fig. 13. On the other hand, there was around 57% of cells with caspase 3/7 positive after treatment with BBC. The combination group showed the most activation in caspase 3/7 where essentially all cells were caspase positive, when compared to the Cu(II) complex or BBC alone.

Caspase 3/7 was also detected by using Caspase-Glo® 3/7 luminescence assay. The cancer cells were treated with the $IC_{50}$ value of the Cu(II) complex and/or BBC for 24 h. The results showed an activation in caspase 3/7 with the single and co-treatment of the Cu(II) complex and BBC. However, the combination group showed the most activation in caspase 3/7 when compared with either the complex or BBC alone as shown in Fig. 14. These results indicate the induction of apoptotic cell death mechanism in MDA-MB-231 VIM RFP cells with the complex and/or BBC treatment. According to recent studies, berberine induced apoptosis and inhibited cancer cell growth in a variety of cell lines [45-47]. A study by Hwang *et al.* [48] reported the inhibition of proliferation and markedly induction of apoptosis after treatment with berberine in human hepatoma cells [48]. In this work, we have shown that the combination of berberine and the Cu(II) complex was able to enhance the apoptotic rate in TNBC cells.

**Caspase 8 and 9 activities.—**Caspase 8 and 9 activities were studied to investigate which apoptotic pathway was induced after treatment with the compounds. The cancer cells were treated with the $IC_{50}$ values of the Cu(II) complex and/or BBC for 24 h, then caspase 8 and 9 activities were measured by using Caspase-Glo® 8 and Caspase-Glo® 9 assays. The results showed a significant increase in caspase 8 activity after treatment with BBC and combination treatment group as well (see Fig. 15). This indicates the induction of the extrinsic apoptotic pathway to kill cancer cells. While the results did not show an activation in caspase 8 after treatment with the Cu(II) complex. However, the Cu(II) complex showed activation in caspase 9 indicating the induction of the intrinsic apoptotic pathway. The combination group also showed activation in caspase 9, however, the apoptotic rates induced by the Cu(II) complex and BBC combination were significantly higher than that by either the complex or BBC alone.

**Necroptotic mode of cell death.—**Necroptosis is a programmed form of necrosis showing similar morphological features [49]. Necroptosis is triggered by the activation of death receptors, such FAS and TNF [50]. Necroptosis critically depends on the sequential activation of receptor-interacting serine/threonine kinase 3 (RIPK3) and mixed lineage kinase domain-like pseudokinase (MLKL) [51]. Necroptosis is activated by the binding of TNF ligand to its receptor. When necroptotic pathway initiated, the RIPK1 and RIPK3 auto- and *trans*-phosphorylate each other, leading to the formation of necrosome. The necrosome then phosphorylates the MLKL protein, which then can insert into the plasma membrane and cause the expulsion of cell contents into the extracellular space, resulting in the necrosis phenotype [52,53]. It has been documented that transition metal complexes can cause necroptosis in cancer cells. For example, cisplatin has been reported to induce necroptosis by the activation of TNFα-mediated RIPK1/RIPK3/MLKL pathway [54]. An additional study revealed that several natural products, including neoalbaconol, shikonin, and tea polyphenols, promoted the necroptosis mechanism in cancer cells [55].

**Immunofluorescence study.—**To see whether the Cu(II) complex and BBC affected necroptosis in MDA-MB-231 VIM RFP cells, the activation of RIPK3 and MLKL as biomarkers of necroptosis was detected by using the immunofluorescent assay. The cancer cells were treated with the $IC_{50}$ values of the Cu(II) complex and/or BBC. The proteins were detected by adding p-RIPK3 and p-MLKL primary antibodies. The phosphorylation of RIPK3 (p-RIPK3) and MLKL (p-MLKL) was observed in the Cu(II) complex-treated group as shown by immunoblotting when compared with the untreated group (see Fig. 16). The combination treatment of the Cu(II) complex and BBC induced more necroptotic cells, while the results showed a weak signal in the BBC-treated group. The treatment with BBC suggests the induction of another cell death mechanism to kill cancer cells. The activation of caspase 8 with BBC based on our results could be a reason for the observation of the low p-RIPK3 and p-MLKL, because of the inhibition of RIPK3 by active caspase 8. On the other hand, the data indicates the induction of a necroptotic cell death mechanism *via* the activation of the RIPK3–MLKL pathway after treatment with the combination of the Cu(II) complex and BBC. A previous study showed significant anti-cancer activity of berberine in combination with cisplatin in ovarian cancer cells. This combination therapy caused a high rate of necroptosis suggesting the potential of berberine when combined with another chemotherapeutic agent in the treatment of ovarian cancer [36].

**Western blot study.—**To confirm the results of the activation of necroptotic cell death mechanism with the Cu(II) complex and/or BBC, we used western blot assay to detect the phosphorylation of MLKL biomarker. The results showed activation of MLKL with the combination therapy, while its activation was less detected in the cancer cells treated with the Cu(II) complex or BBC alone as shown in Fig. 17. This is comparable to the results of the immunofluorescence assay. The GAPDH protein was used as a reference. The relative protein level was obtained by comparison with the GAPDH level. The results showed a low level of p-MLKL with BBC treatment, suggesting that BBC induced a low necroptotic rate in TNBC cells with its possibility to induce another cell death mechanism. The Cu(II) complex showed an increase in p-MLKL level when compared to the untreated

group, indicating the activation of necroptosis. However, the combination treatment showed the most activation of necroptosis with a stronger intensity band in the gel.

### Conclusions

Our data on the combination of BBC and the Cu(II) complex had a prominent inhibitory on breast cancer cells. The $IC_{50}$ values in cancer cells for the Cu(II) complex, BBC, and combination treatment were 21.2 ± 1.6, 48.3 ± 2.4, and 9.3 ± 1.5 μM, respectively. The combination treatment successfully reduced the cytotoxic effect on the non-cancer MCF-10A cells. The $IC_{50}$ values of the Cu(II) complex in combination with 50 μM of BBC was 94.5 ± 1.8 μM in non-cancer cells compared to 9.3 ± 1.5 μM in cancer cells, indicating the selectivity of the combination therapy. From the data acquired *via* cell death mechanism studies, the results showed activation of the intrinsic apoptotic pathway with the Cu(II) complex and the extrinsic pathway with BBC. Targeting of different apoptotic pathways by each compound is suggested to be a reason for the enhancement of the anti-cancer effect that occurs with the combination treatment.

In the necroptosis study, the combination treatment exhibited the most induction of necroptosis as showed an increase in MLKL phosphorylation level when compared to the treatment with BBC or the Cu(II) complex alone. Moreover, the Cu(II) complex showed a significant cell cycle arrest in the S phase, while BBC inhibited the cell cycle in G2 phase. On the other hand, the combination treatment caused a greater number of cells arrested in the G2 phase preventing cancer cell division.

The data suggest that BBC in the co-treatment group increased the DNA damage in the S phase which is induced by the Cu(II) complex leading to an increase in the suppression of MDA-MB-231 VIM RFP cancer cells. We found that the co-treatment group enhanced cancer cell death by inducing apoptosis through the caspase-dependent pathway and necroptosis through the RIPK3-MLKL pathway, which could improve the anti-cancer effects of chemotherapeutic drugs. This finding may provide insight into the potential use of the copper(II) complex in the treatment of TNBC and a new therapeutic strategy when the complex is combined with BBC for the clinical treatment of TNBC in the future.

## Supplementary Material

Refer to Web version on PubMed Central for supplementary material.

## Acknowledgements

Research reported in this publication was supported by the National Institute Of General Medical Sciences of the National Institutes of Health under Award Number T34GM149392. The content is solely the responsibility of the authors and does not necessarily represent the official views of the National Institutes of Health.

C.L. would like to thank the National Science Foundation (NSF) for the Department of Chemistry and Biochemistry's REU site as this material is based upon work supported by the National Science Foundation under CHE-2150385.

Research reported in this publication was supported by National Institute of General Medical Sciences (NIGMS) of the National Institutes of Health under award 1T34GM149816. Matching funds from Old Dominion University are also acknowledged.

This work was also supported by a Saudi Arabian Cultural Mission (SACM) scholarship to DRA. The authors are also grateful for the suggestions made by the reviewers.

## Data availability

Data will be made available on request.

## Abbreviations:

| | |
|---|---|
| **CCK-8 assay** | Cell Counting Kit-8 |
| **DMEM** | Dulbecco's Modified Eagle Medium |
| **DAPI** | 4′,6-diamidino-2-phenylindole |
| **EMEM** | Eagle's Minimum Essential Medium |
| **EGF** | Epidermal growth factor |
| **FBS** | Fetal bovine serum |
| **GADPH** | Glyceraldehyde 3-phosphate dehydrogenase |
| **HER2** | Human epidermal growth factor receptor 2 |
| **MLKL** | Mixed lineage kinase domain-like pseudokinase |
| **RFP** | Red fluorescent protein |
| **RIPK3** | Receptor-interacting serine/threonine-protein kinase 3 |
| **TNBC** | Triple negative breast cancer |
| **TSCs** | Thiosemicarbazones |
| **VIM** | Vimentin |
| **WST-8** | [2-(2-methoxy-4-nitrophenyl)-3-(4-nitrophenyl)- 5-(2,4-disulfophenyl)-2H-tetra zolium, monosodium salt |

## References

[1]. Ismail-Khan R, Bui MM, Cancer Control 17 (2010) 173–176. [PubMed: 20664514]

[2]. Bertucci F, Finetti P, Cervera N, Esterni B, Hermitte F, Viens P, Birnbaum D, Int. J. Cancer 123 (2008) 236–240. [PubMed: 18398844]

[3]. Kassam F, Enright K, Dent R, Dranitsaris G, Myers J, Flynn C, Fralick M, Kumar R, Clemons M, Clin. Breast Cancer 9 (2009) 29–33. [PubMed: 19299237]

[4]. Liu Y-R, Jiang Y-Z, Xu X-E, Hu X, Yu K-D, Shao Z-M, Clin. Cancer Res. 22 (2016) 1653–1662. [PubMed: 26813360]

[5]. Morris GJ, Naidu S, Topham AK, Guiles F, Xu Y, McCue P, Schwartz GF, Park PK, Rosenberg AL, Brill K, Cancer 110 (2007) 876–884. [PubMed: 17620276]

[6]. Dent R, Trudeau M, Pritchard KI, Hanna WM, Kahn HK, Sawka CA, Lickley LA, Rawlinson E, Sun P, Narod SA, Clin. Cancer Res 13 (2007) 4429–4434. [PubMed: 17671126]

[7]. Zhang L, Fang C, Xu X, Li A, Cai Q, Long X, BioMed Res. Int 2015 (2015).

[8]. Gluz O, Liedtke C, Gottschalk N, Pusztai L, Nitz U, Harbeck N, Ann. Oncol 20 (2009) 1913–1927. [PubMed: 19901010]

[9]. Iakovidis I, Delimaris I, Piperakis SM, Mol. Biol. Int 2011 (2011).

[10]. Metzler-Nolte N, Kraatz H, Concepts and models in bioinorganic chemistry, Wiley-VCH. (2006).

[11]. Ruiz-Azuara L, Bravo-Gomez ME, Curr. Med. Chem 17 (2010) 3606–3615. [PubMed: 20846116]

[12]. Hernández-Esquivel L, Marín-Hernández A, Pavón N, Carvajal K, Moreno-Sánchez R, Toxicol. Appl. Pharmacol 212 (2006) 79–88. [PubMed: 16051288]

[13]. Rivero-Müller A, De Vizcaya-Ruiz A, Plant N, Ruiz L, Dobrota M, Chem. Biol. Interact 165 (2007) 189–199. [PubMed: 17217939]

[14]. Trejo-Solís C, Palencia G, Zúniga S, Rodríguez-Ropon A, Osorio-Rico L, Luvia ST, Gracia-Mora I, Marquez-Rosado L, Sánchez A, Moreno-García ME, Neoplasia 7 (2005) 563–574. [PubMed: 16036107]

[15]. Liedtke C, Mazouni C, Hess KR, André F, Tordai A, Mejia JA, Symmans WF, Gonzalez-Angulo AM, Hennessy B, Green M, J. Clin. Oncol 26 (2008) 1275–1281. [PubMed: 18250347]

[16]. Pagani M, Bavbek S, Dursun AB, Bonadonna P, Caralli M, Cernadas J, Cortellini G, Costantino MT, Gelincik A, Lucchini G, J. Clin. Immunol 7 (2019) 990–997.

[17]. Edwardson DW, Narendrula R, Chewchuk S, Mispel-Beyer K, Mapletoft JPJ, Parissenti AM, Curr. Drug Metab 16 (2015) 412–426. [PubMed: 26321196]

[18]. Yap TA, Omlin A, De Bono JS, J. Clin. Oncol 31 (2013) 1592–1605. [PubMed: 23509311]

[19]. Albain KS, Nag SM, Calderillo-Ruiz G, Jordaan JP, Llombart AC, Pluzanska A, Rolski J, Melemed AS, Reyes-Vidal JM, Sekhon JS, J. Clin. Oncol 26 (2008) 3950–3957. [PubMed: 18711184]

[20]. Blagosklonny MV, Trends Pharmacol. Sci 26 (2005) 77–81. [PubMed: 15681024]

[21]. Qiu M, Xue C, Zhang L, J. BUON 24 (2019) 2316–2321. [PubMed: 31983100]

[22]. Letašiová S, Jantová S, Miko M, Ovádeková R, Horváthová M, J. Pharm. Pharmacol 58 (2006) 263–270. [PubMed: 16451756]

[23]. Wang N, Feng Y, Zhu M, Tsang CM, Man K, Tong Y, Tsao SW, J. Cell. Biochem 111 (2010) 1426–1436. [PubMed: 20830746]

[24]. Fukuda K, Hibiya Y, Mutoh M, Koshiji M, Akao S, Fujiwara H, J. Ethnopharmacol 66 (1999) 227–233. [PubMed: 10433483]

[25]. Youn M-J, So H-S, Cho H-J, Kim H-J, Kim Y, Lee J-H, Sohn JS, Kim YK, Chung S-Y, Park R, Biol. Pharm. Bull 31 (2008) 789–795. [PubMed: 18451495]

[26]. Zhao Y, Jing Z, Li Y, Mao W, Oncol. Rep 36 (2016) 567–572. [PubMed: 27177238]

[27]. Haribabu J, Srividya S, Mahendiran D, Gayathri D, Venkatramu V, Bhuvanesh N, Karvembu R, Inorg. Chem 59 (2020) 17109–17122. [PubMed: 33231439]

[28]. Balakrishnan N, Haribabu J, Dhanabalan AK, Swaminathan S, Sun S, Dibwe DF, Bhuvanesh N, Awale S, Karvembu R, Dalton Trans. 49 (2020) 9411–9424. [PubMed: 32589180]

[29]. Li Y, Yang Z-Y, Wu J-C, Eur. J. Med. Chem 45 (2010) 5692–5701. [PubMed: 20884087]

[30]. Kalaiarasi G, Rajkumar SRJ, Dharani S, Lynch VM, Prabhakaran R, Inorg. Chim. Acta 471 (2018) 759–776.

[31]. Geary WJ, Coord. Chem. Rev 7 (1971) 81–122.

[32]. Beckford FA, Shaloski M Jr., Leblanc G, Thessing J, Lewis-Alleyne LC, Holder AA, Li L, Seeram NP, Dalton Trans. (2009) 10757–10764. [PubMed: 20023905]

[33]. Beckford FA, Thessing J, Stott A, Holder AA, Poluektov OG, Li L, Seeram NP, Inorg. Chem. Commun 15 (2012) 225–229. [PubMed: 23440300]

[34]. Sandhaus S, Taylor R, Edwards T, Huddleston A, Wooten Y, Venkatraman R, Weber RT, González-Sarrías A, Martin P, Cagle P, Tse-Dinh YC, Beebe SJ, Seeram N, Holder AA, Inorg. Chem. Commun 64 (2016) 45–49. [PubMed: 26752972]

[35]. Zhao Y, Jing Z, Lv J, Zhang Z, Lin J, Cao X, Zhao Z, Liu P, Mao W, Biomed. Pharmacother 95 (2017) 18–24. [PubMed: 28826092]

[36]. Liu L, Fan J, Ai G, Liu J, Luo N, Li C, Cheng Z, Biol. Res 52 (2019) 1–14. [PubMed: 30612577]

[37]. Mantena SK, Sharma SD, Katiyar SK, Mol. Cancer Ther 5 (2006) 296–308. [PubMed: 16505103]

[38]. Jahnke GD, Price CJ, Marr MC, Myers CB, George JD, Birth Defects Res, B Dev. Reprod. Toxicol 77 (2006) 195–206. [PubMed: 16634078]

[39]. Hedrick CC, Malanchi I, Nat. Rev. Immunol 22 (2022) 173–187. [PubMed: 34230649]

[40]. Lu W, Du S, Wang J, Mol. Med. Rep 11 (2015) 3920–3924. [PubMed: 25572870]

[41]. Zhang H, Thomas R, Oupicky D, Peng F, J. Biol. Inorg. Chem 13 (2008) 47–55. [PubMed: 17909866]

[42]. Thelander L, Gräslund A, J. Biol. Chem 258 (1983) 4063–4066. [PubMed: 6300073]

[43]. Kaska WC, Carrano C, Michalowski J, Jackson J, Levinson W, Bioinorg. Chem 8 (1978) 245–254. [PubMed: 647057]

[44]. Mahendiran D, Amuthakala S, Bhuvanesh NS, Kumar RS, Rahiman AK, RSC Adv. 8 (2018) 16973–16990. [PubMed: 35540520]

[45]. Jantova S, Cipak L, Letasiova S, Toxicol. in Vitro 21 (2007) 25–31. [PubMed: 17011159]

[46]. Čerňáková M, Košt'álová D, Kettmann V, Plodová M, Tóth J, Dřímal J, Complement BMC, Altern. Med 2 (2002) 1–6.

[47]. Jantova S, Cipak L, Cernakova M, Kostalova D, J. Pharm. Pharmacol 55 (2003) 1143–1149. [PubMed: 12956905]

[48]. Hwang J-M, Kuo H-C, Tseng T-H, Liu J-Y, Chu C-Y, Arch. Toxicol 80 (2006) 62–73. [PubMed: 16189662]

[49]. Pasparakis M, Vandenabeele P, Nature 517 (2015) 311–320. [PubMed: 25592536]

[50]. Linkermann A, Green DR, N. Engl, J. Med 370 (2014) 455–465. [PubMed: 24476434]

[51]. Murphy JM, Czabotar PE, Hildebrand JM, Lucet IS, Zhang J-G, Alvarez-Diaz S, Lewis R, Lalaoui N, Metcalf D, Webb AI, Immunity 39 (2013) 443–453. [PubMed: 24012422]

[52]. Berghe TV, Linkermann A, Jouan-Lanhouet S, Walczak H, Vandenabeele P, Nat. Rev. Mol. Cell Biol 15 (2014) 135–147. [PubMed: 24452471]

[53]. Wang H, Sun L, Su L, Rizo J, Liu L, Wang L-F, Wang F-S, Wang X, Mol. Cell 54 (2014) 133–146. [PubMed: 24703947]

[54]. Xu Y, Ma H-B, Fang Y-L, Zhang Z-R, Shao J, Hong M, Huang C-J, Liu J, Chen R-Q, Cell. Signal 31 (2017) 112–123. [PubMed: 28065786]

[55]. Yu J, Zhong B, Xiao Q, Du L, Hou Y, Sun H-S, Lu J-J, Chen X, Pharm. Ther 214 (2020) 107593.

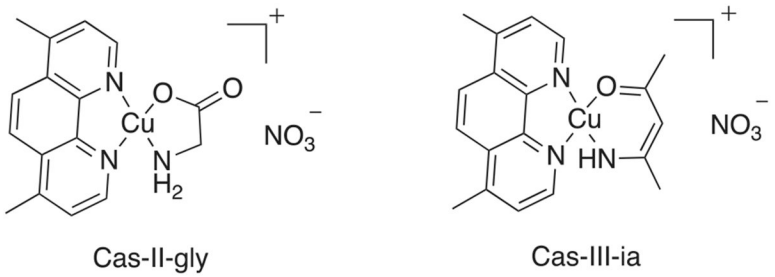


**Fig. 1.**
Structures of representative Casiopeinas complexes [14].

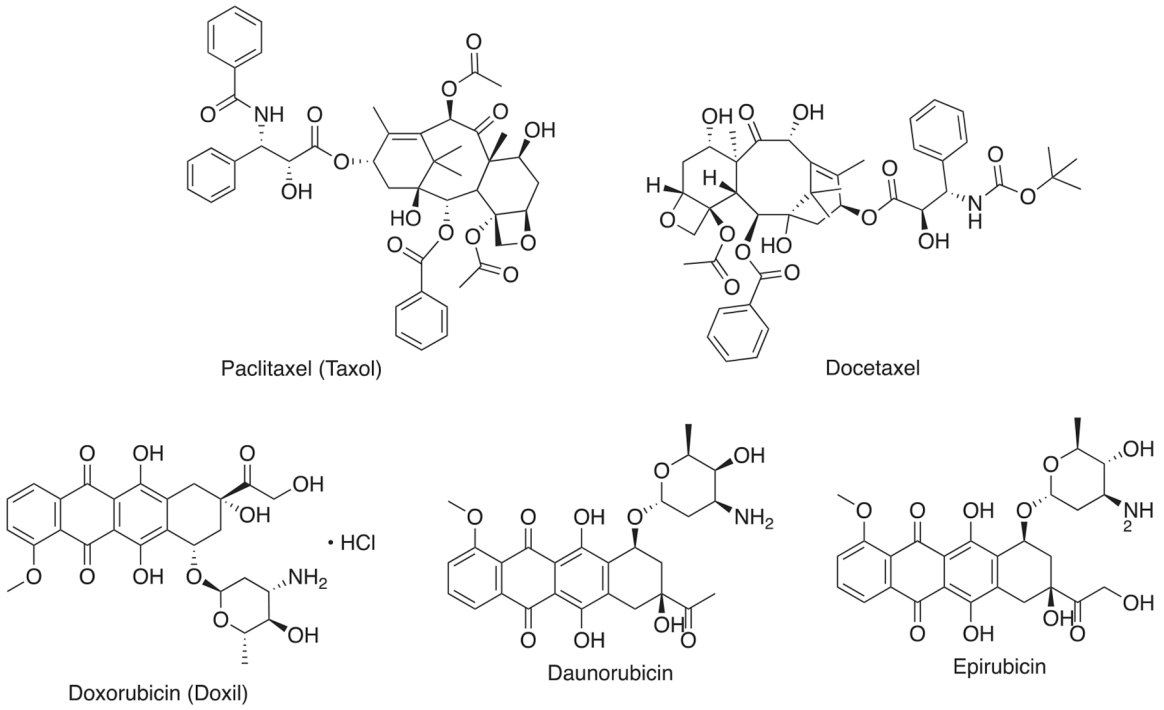


**Fig. 2.**
Structures of some chemotherapeutic drugs used for patients with TNBC.

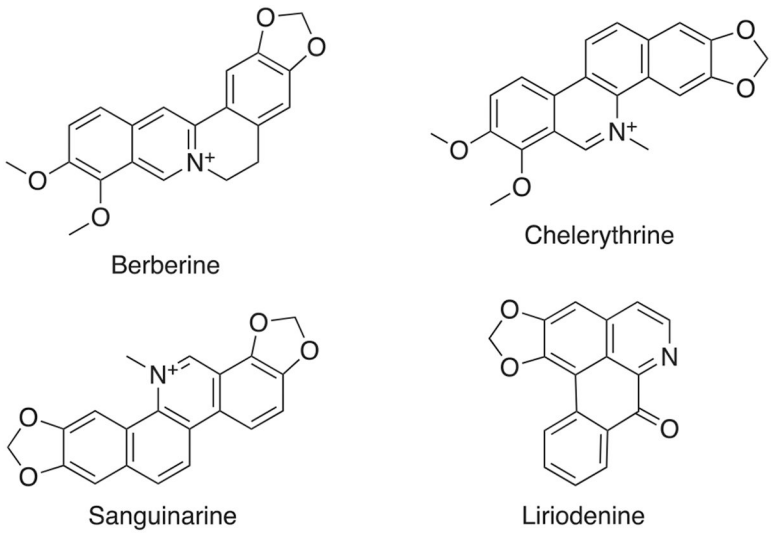


**Fig. 3.**
Representative examples of isoquinoline alkaloids.

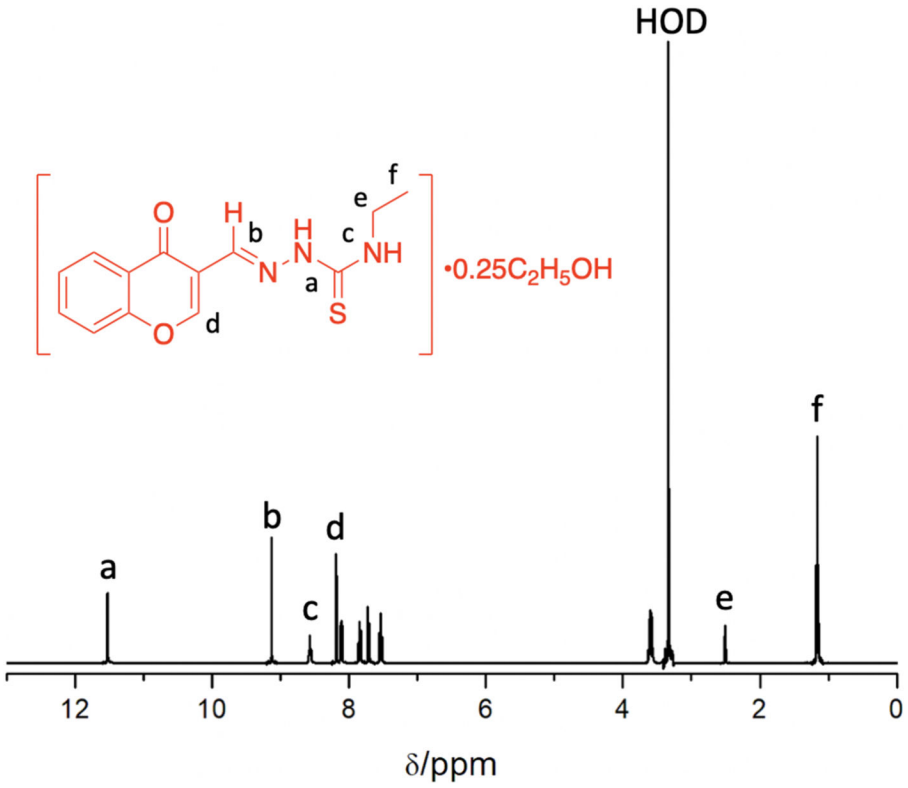


**Fig. 4.**
$^{1}$H NMR spectrum of the chromoneTSC•0.25$C_2H_5OH$ ligand in DMSO-$d_6$.

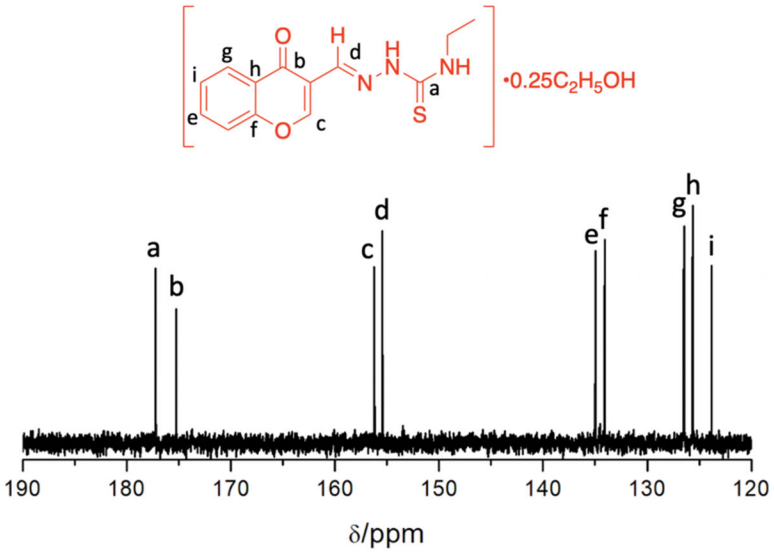


**Fig. 5.**

$^{13}$C NMR spectrum of the chromoneTSC•0.25$C_2H_5OH$ ligand in DMSO-$d_6$.

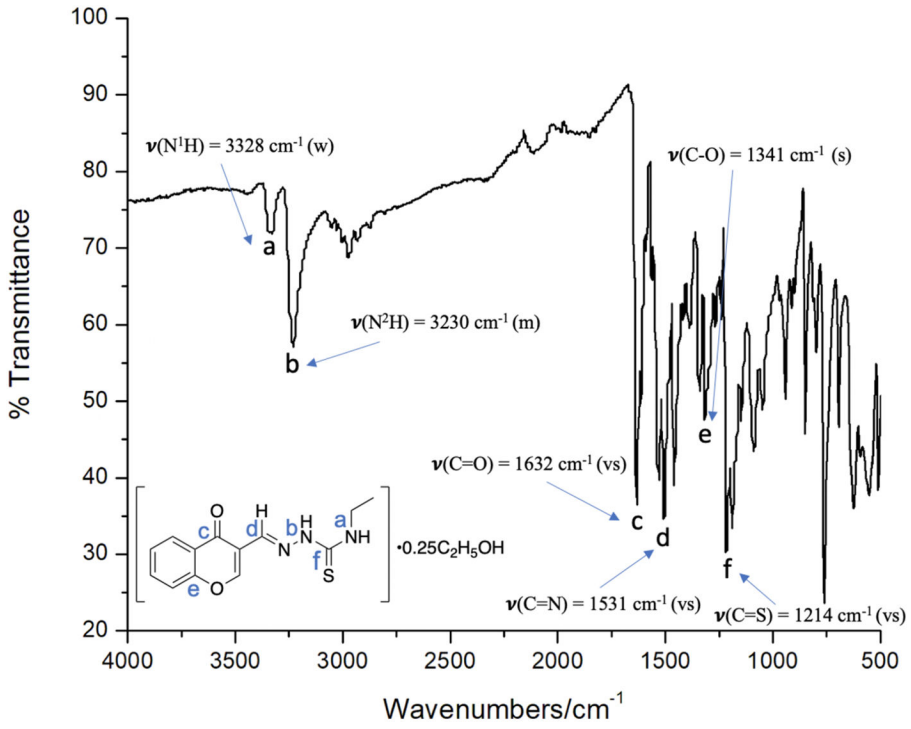


**Fig. 6.**

FTIR spectrum of the chromoneTSC•0.25$C_2H_5OH$ ligand.

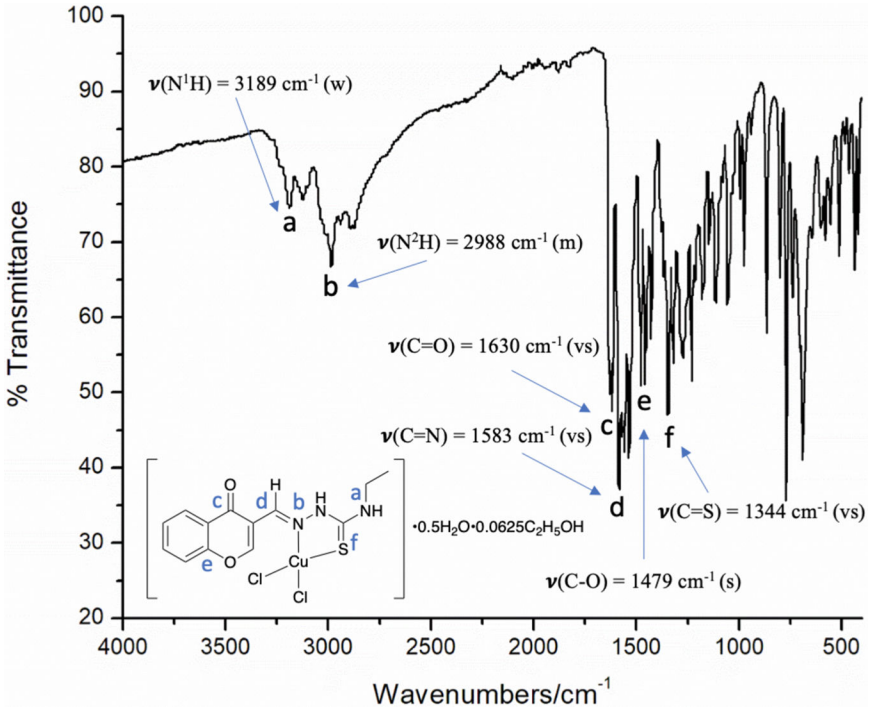


**Fig. 7.**
FTIR spectrum of the copper(II) complex.

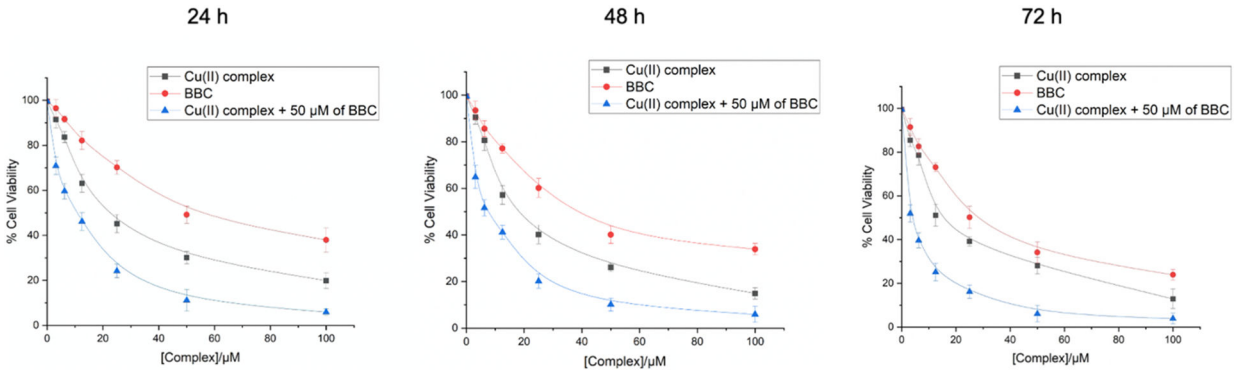


**Fig. 8.**

A plot of the percentage of MDA-MB-231 VIM RFP cell viability versus concentration of the copper(II) complex and/or berberine chloride (BBC) at 24, 48, and 72 h incubation.

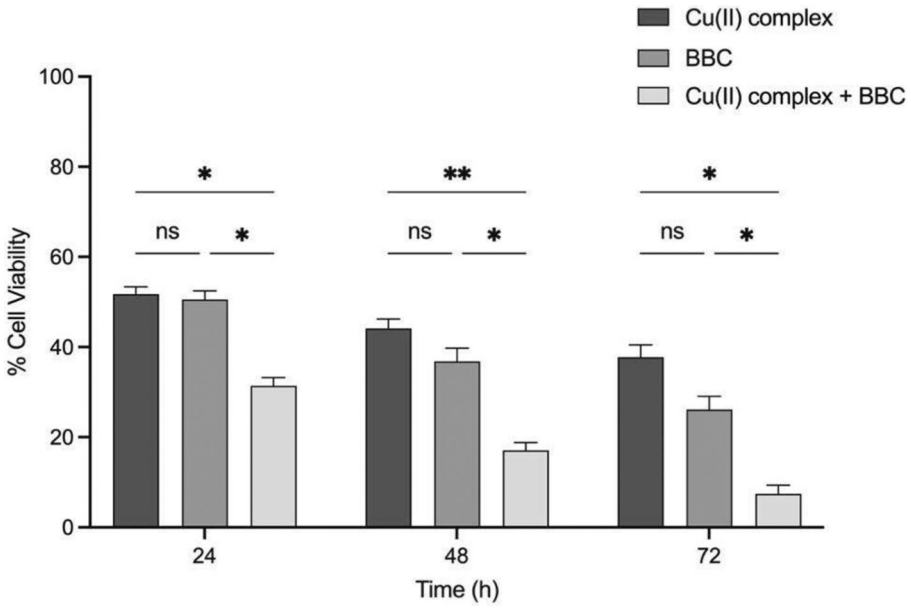


**Fig. 9.**

Cancer MDA-MB-231 VIM RFP cell viability after treatment with the copper(II) complex (20 μM) and/or berberine chloride, BBC, (50 μM) at 24, 48, and 72 h incubations. Cell viability was measured by CCK-8 assay. Data were based on at least three independent experiments, and shown as mean ± SD. The results were analyzed using GraphPad Prism software (*$p < 0.05$, **$p < 0.01$).

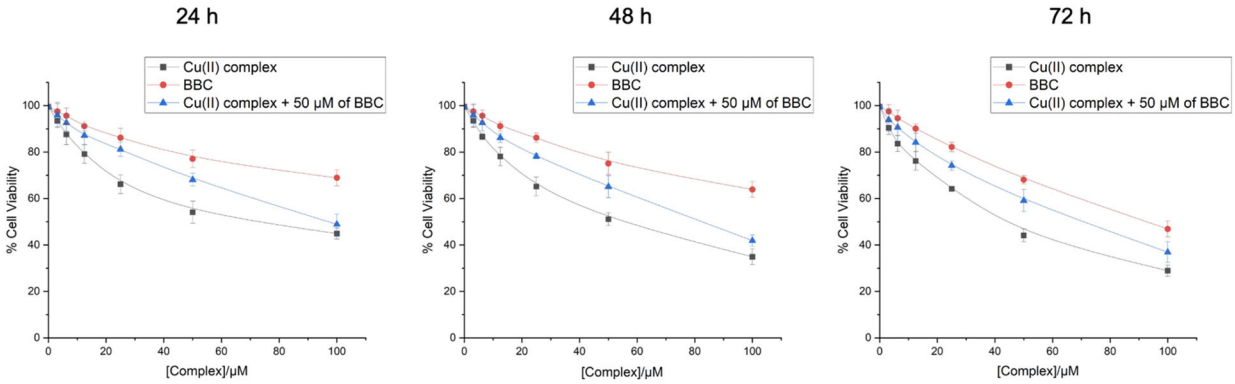


**Fig. 10.**

A plot of the percentage of MCF-10A cell viability versus concentration of the copper(II) complex and/or berberine chloride (BBC) at 24, 48, and 72 h incubation.

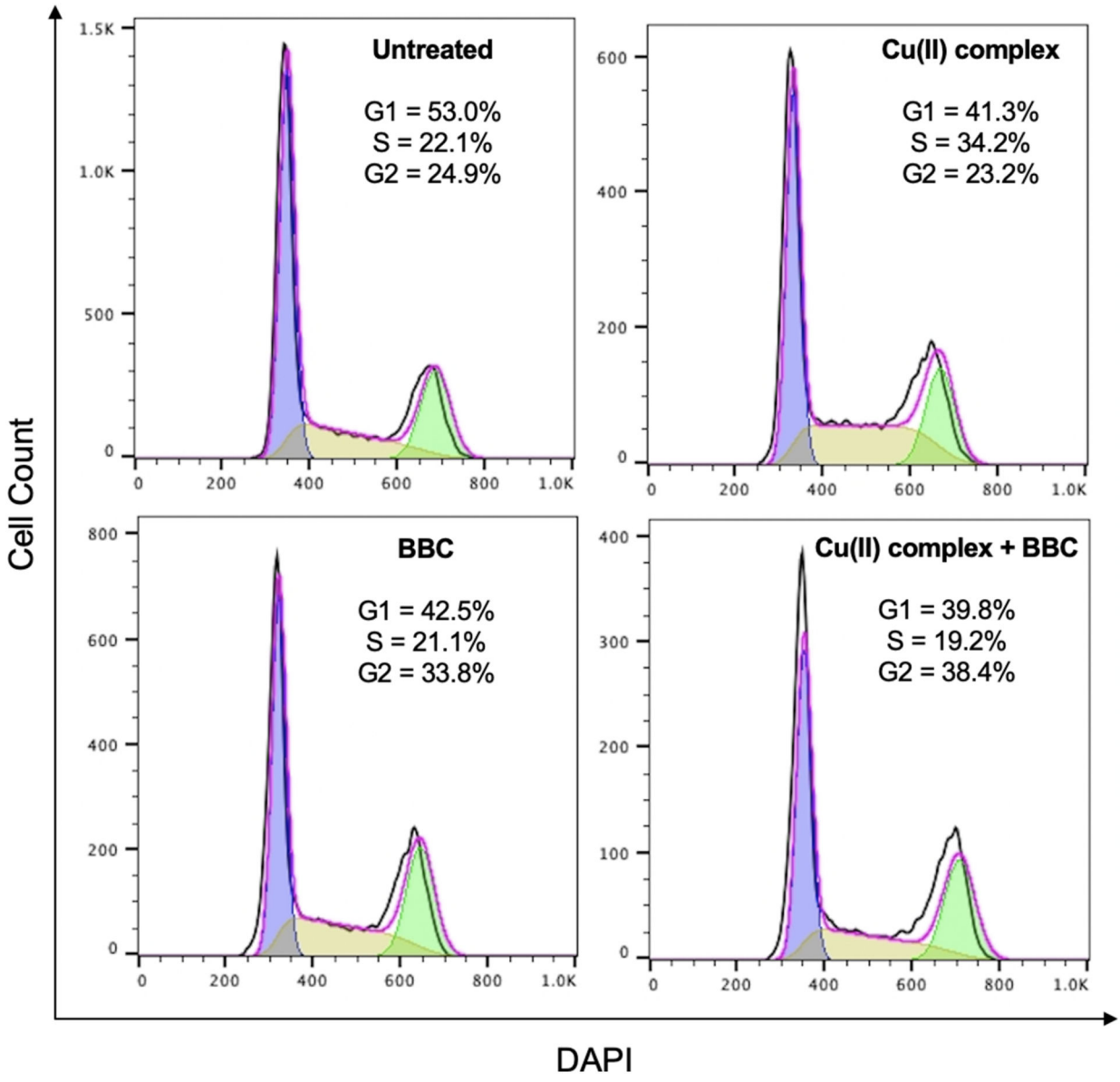


**Fig. 11.**

Cell cycle results after treatment with the copper(II) complex and/or berberine chloride (BBC) for 24 h. The MDA-MB-231 VIM RFP cells were plated at a density of $1 \times 10^6$ in 6-well plate. The cells were treated with the complex (20 μM) and/or BBC (50 μM) for 24 h. The cell cycle was evaluated by flow cytometry using DAPI staining. The blue DAPI florescent was read at 450/50 nm. Experiments were performed in triplicate. The fractions of cell cycle (G1, S, and G2) were quantified with the FlowJo software.

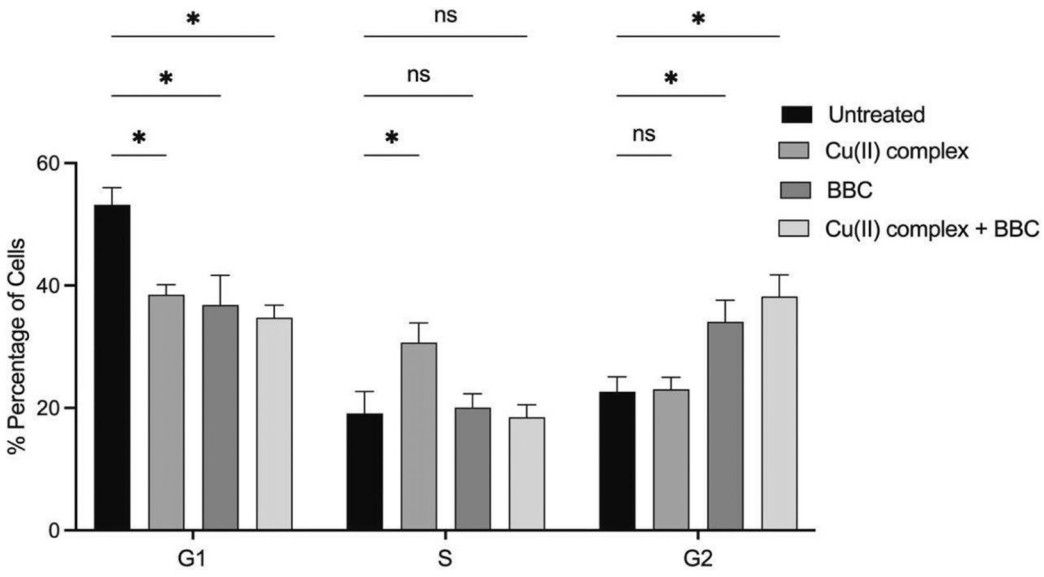


**Fig. 12.**

Quantified results representing fractions of cell cycle (G1, S, and G2) in MDA-MB-231 VIM RFP cells after treatment with the copper(II) complex and/or berberine chloride (BBC) for 24 h. Experiments were performed in triplicate. The results were analyzed using GraphPad Prism software. (Data presented as mean + std. err. *$p < 0.05$, **$p < 0.01$).

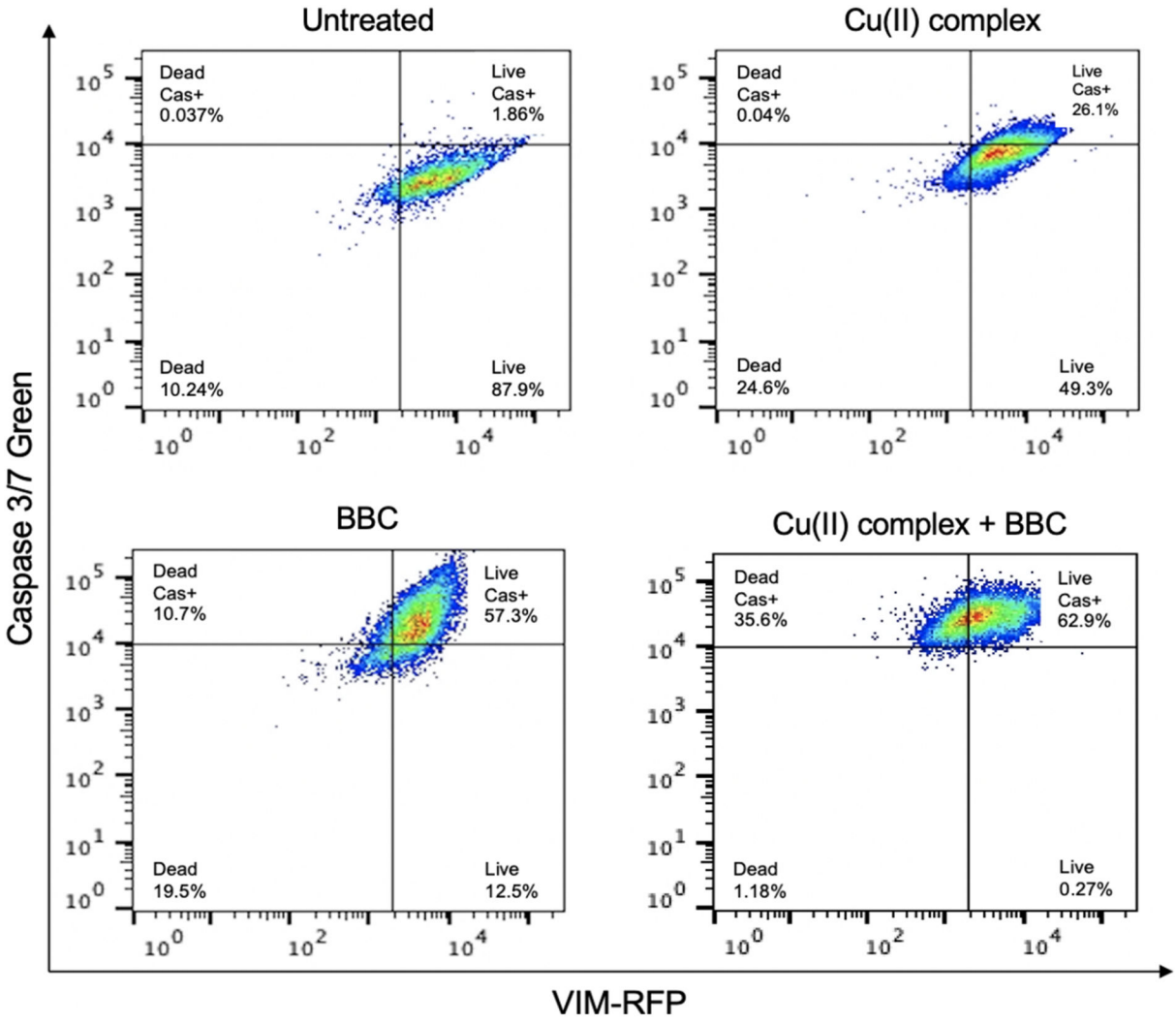


**Fig. 13.**

Caspase 3/7 activity in the MDA-MB-231 VIM RFP cells after treatment with the copper(II) complex and/or berberine chloride (BBC) for 24 h. The cells were seeded at a concentration of $3 \times 10^5$ cells/mL following the treatment with the $IC_{50}$ values of compounds. After 24 h of treatment, the caspase 3/7 reagent was added. The graph shows the population of cells that were activated by caspase 3/7 through collecting the RFP fluorescent at 532/588 and the caspase 3/7 green fluorescent at 511/533 nm by flow cytometry. FlowJo software was used for analyzing flow cytometric data.

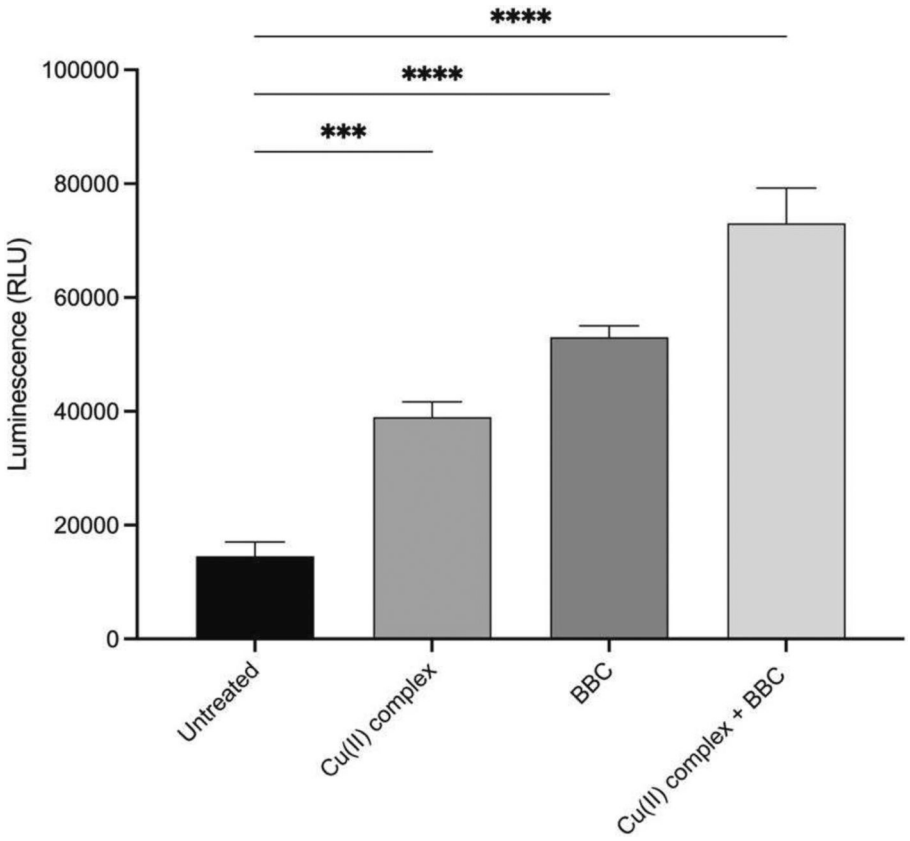


**Fig. 14.**

Caspase 3/7 activity in the MDA-MB-231 VIM RFP cells after treatment with the copper(II) complex and/or berberine chloride (BBC) for 24 h. The cells were seeded at a density of 1.5 × $10^4$ cells per well followed by adding the $IC_{50}$ value of the complex (20 μM) and/or BBC (50 μM) for 24 h. Caspase 3/7 activity was measured by reading the luminescence. Values represent the mean ± SE (n = 3), and data were analyzed using GraphPad Prism 9.

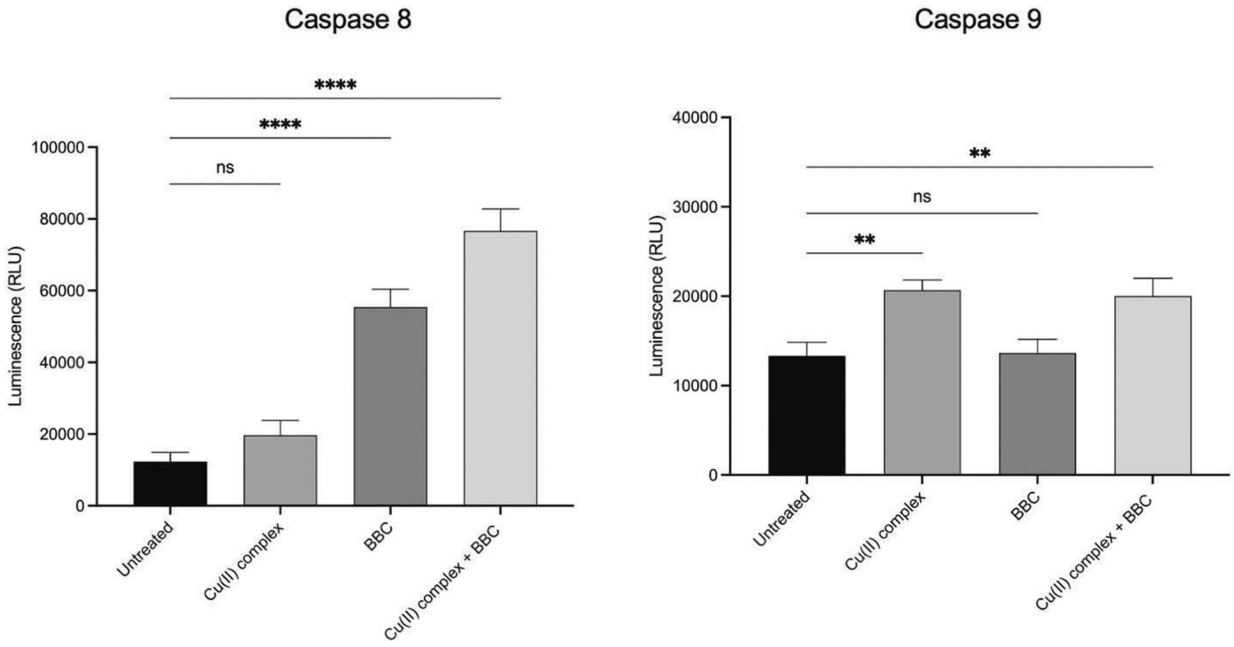


**Fig. 15.**

Caspase 8 and caspase 9 activities, respectively in the MDA-MB-231 VIM RFP cells after treatment with the copper(II) complex and/or berberine chloride (BBC) for 24 h by using a luminescent assay.

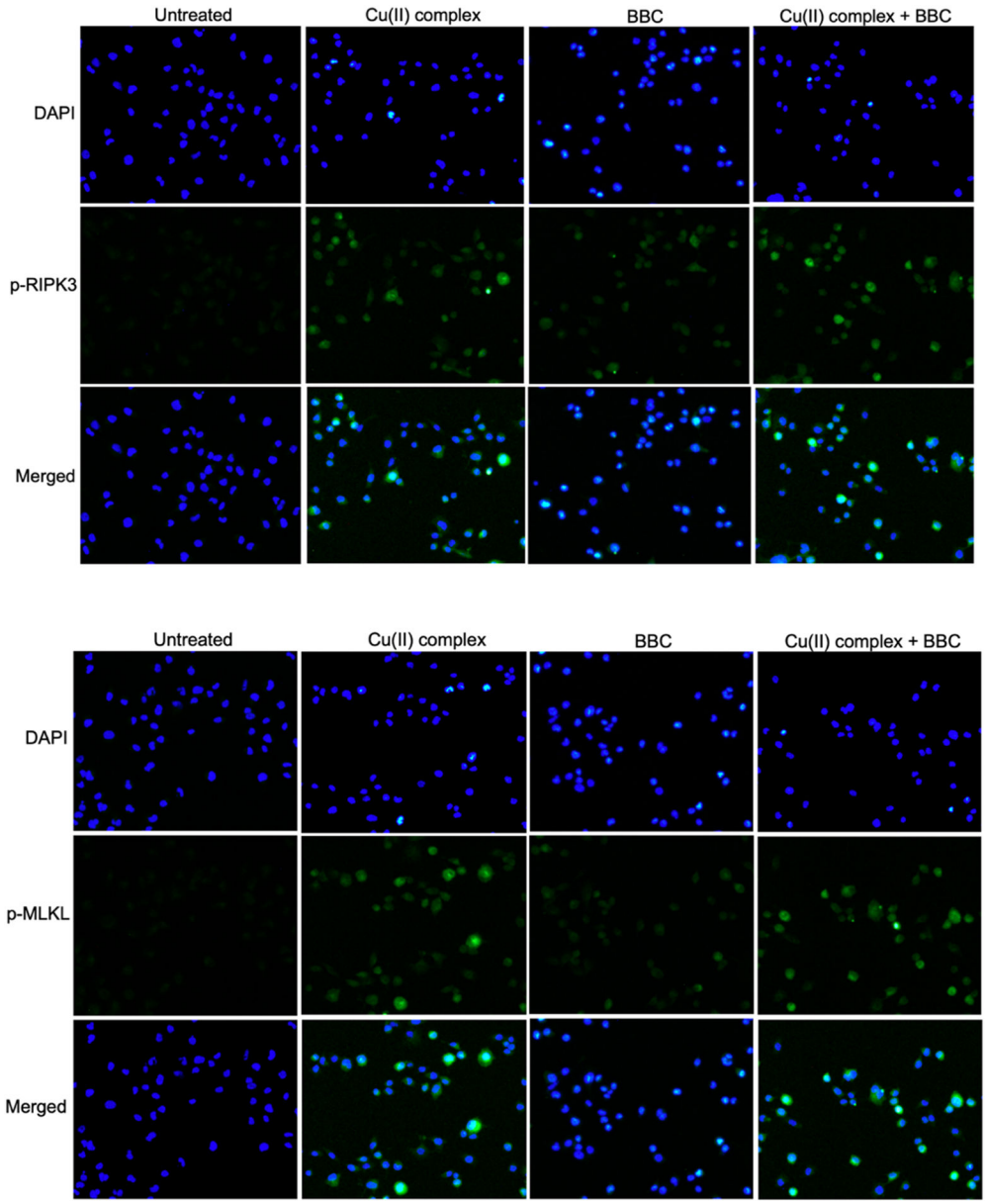


**Fig. 16.**

RIPK3 and MLKL activities after treatment with copper(II) complex and/or berberine chloride (BBC) for 24 h using the immunofluorescence assay. The cancer cells were plated in 4-well chamber slides and treated with the $IC_{50}$ values of the complex (20 μM) and/or BBC (50 μM). p-RIPK3 and p-MLKL primary antibodies were added and incubated at 4 °C overnight. The cells were incubated with the Alexa Fluor™ Plus 488 secondary antibody at room temperature for 1 h. Images were obtained with a fluorescence microscope.

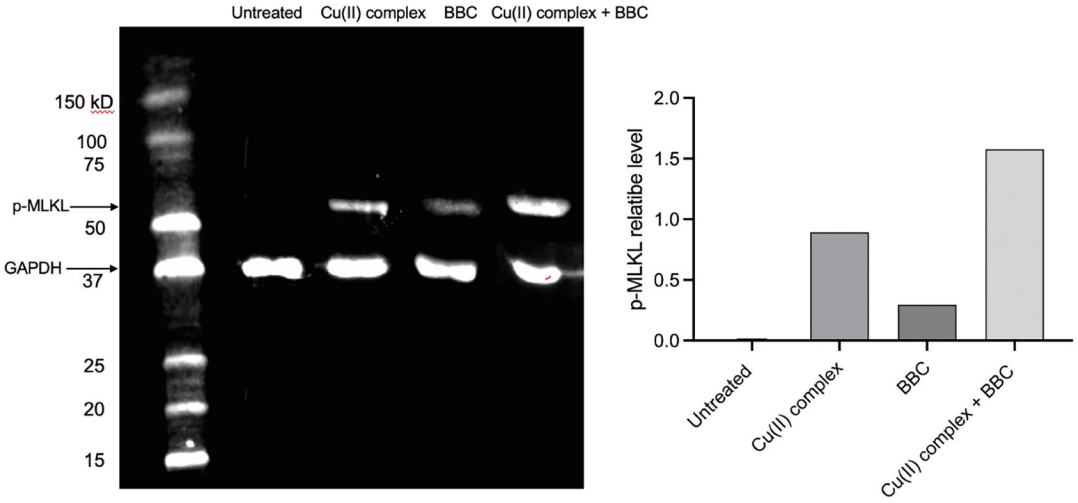


**Fig. 17.**

MLKL activity after treatment with complex 3 and/or berberine chloride (BBC) for 24 h using western blot assay. The cancer cells were treated with the $IC_{50}$ values of complex 3 (20 μM) and/or BBC (50 μM). The extracted proteins were loaded and separated in 10% SDS-PAGE gel. p-MLKL and GAPDH primary antibodies were added and incubated at 4 °C overnight. The cells were incubated with the secondary Alexa Fluor™ Plus 488 antibody for 1 h. Data were analyzed by using Imaged software.

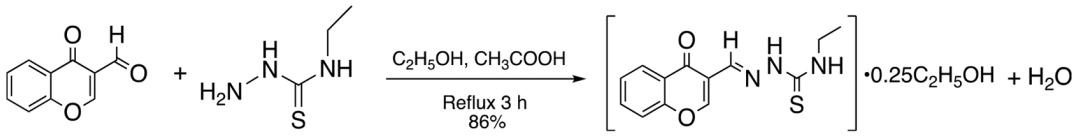


**Scheme 1.**
Synthesis of chromoneTSC•0.25$C_2H_5OH$.

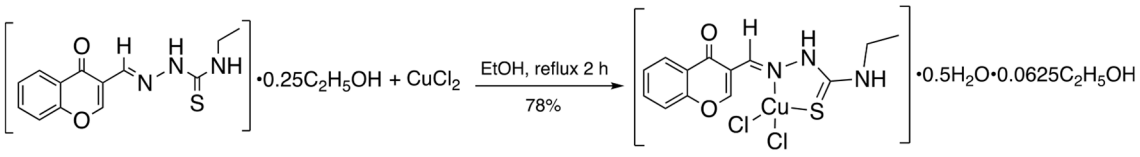


**Scheme 2.**
Synthesis of the copper(II) complex.

**Table 1**

FTIR spectroscopic data for the “free” ligand and the complex ($cm^{-1}$).

| Species | $\nu(N^1H)$ | $\nu(N^2H)$ | $\nu(C=O)$ | $\nu(C=N)$ | $\nu(C\text{-}O)$ | $\nu(C=S)$ |
|---|---|---|---|---|---|---|
| chromoneTSC•0.25$C_2H_5OH$ | 3328 | 3230 | 1632 | 1531 | 1341 | 1214 |
| Copper(II) complex | 3189 | 2988 | 1630 | 1583 | 1479 | 1344 |

*Results Chem*. Author manuscript; available in PMC 2025 January 10.

**Table 2**

Cytotoxic effects of the copper(II) complex in combination with berberine chloride *via* $IC_{50}$ values on MDA-MB-231 VIM RFP cells at different times.

| | **$IC_{50}$ /μM Cancer MDA-MB-231 VIM RFP** | | |
|---|---|---|---|
| | **24 h** | **48 h** | **72 h** |
| Copper(II) complex | 21.2 ± 1.6 | 16.7 ± 2.3 | 12.1 ± 1.7 |
| Berberine chloride (BBC) | 48.3 ± 2.4 | 31.8 ± 2.6 | 25.6 ± 1.9 |
| Copper(II) complex + 50 μM of BBC | 9.3 ± 1.5 | 5.4 ± 2.1 | 3.7 ± 1.6 |
| Cisplatin | 28.13 ± 2.4 | 24.73 ± 2.6 | 22.17 ± 1.8 |

**Table 3**

Cytotoxic effects of the copper(II) complex in combination with berberine chloride *via* $IC_{50}$ values on MCF-10A cells at different times.

| | **$IC_{50}$ /μM Non-cancer MCF-10A** | | |
|---|---|---|---|
| | **24 h** | **48 h** | **72 h** |
| Copper(II) complex | 58.7 ± 2.1 | 51.2 ± 1.7 | 46.3 ± 2.4 |
| Berberine chloride (BBC) | >100 | >100 | 92.3 ± 1.4 |
| Copper(II) complex + 50 μM of BBC | 94.5 ± 1.8 | 84.1 ± 2.2 | 75.4 ± 1.6 |
| Cisplatin | 41.22 ± 1.9 | 34.20 ± 2.7 | ± 2.0 |